

# Spontaneous symmetry breaking of the Ir(100)-(5×1)-hex surface induced by hydrogen adsorption

H. C. Poon and D. K. Saldin\*

Department of Physics and Laboratory for Surface Studies, University of Wisconsin–Milwaukee, P. O. Box 413, Milwaukee, Wisconsin 53201, USA

D. Lerch, W. Meier, A. Schmidt, A. Klein, S. Müller, L. Hammer, and K. Heinz  
 Lehrstuhl für Festkörperphysik, Universität Erlangen–Nürnberg, Staudtstrasse 7, D-91058 Erlangen, Germany  
 (Received 10 March 2006; revised manuscript received 10 July 2006; published 14 September 2006)

A structural study by quantitative low-energy electron diffraction (LEED) and density functional theory (DFT) has been performed on the Ir(100)-(5×1)-hex surface with 0.6 ML of hydrogen adsorbed at low temperature (<180 K). The theory-experiment fit of LEED intensities based on calculations applying the two mirror symmetry planes of the uncovered surface is not satisfactory. Instead, the real structure has a unit cell with only one mirror plane yielding an excellent  $R$  factor ( $R_p=0.16$ ). The DFT investigation of the energetics also confirms this spontaneous symmetry breaking, yields quantitatively the same structure for the substrate as the LEED analysis and, moreover, retrieves the hydrogen positions. It was found that adsorption of hydrogen leads to an asymmetric increase of the buckling of the top hexagonal layer, with one of the previously protruding surface Ir atoms extruded even more by about 0.1 Å. This may be regarded as a precursor of the temperature-activated phase transition above 180 K to a structure in which the most protruding atom of the (5×1) surface unit cell is ejected from the quasihexagonal top layer. These ejected atoms form single-atom-wide iridium wires on the remaining atoms, which rearrange to form a bulklike fcc(100) layer, leading to a complete lifting of the quasihexagonal reconstruction.

DOI: 10.1103/PhysRevB.74.125413

PACS number(s): 61.14.Hg, 68.43.Bc, 68.43.Fg, 68.47.De

## I. INTRODUCTION

Recently, the (5×1) hexagonally reconstructed Ir(100) surface, Ir(100)-(5×1)-hex, has been shown to undergo a substantial structural phase transition when exposed to hydrogen at temperatures above 180 K (Ref. 1). It was demonstrated that the new structure consists of atomically thin and macroscopically long parallel Ir wires separated (on average) by five times the bulk interatomic spacing, i.e., by 1.36 nm on a nearly bulk-terminated, i.e., unreconstructed Ir(100) substrate. It was also demonstrated that this nanostructured Ir(100)-(5×1)-H phase can be used as a template to build other nanostructures by decoration of the Ir wires with, e.g., iron.<sup>2,3</sup> This role of the new Ir phase as a template has caused additional interest in how it is formed upon exposure of the Ir(100)-(5×1)-hex surface to hydrogen at sufficiently high temperatures.

We therefore investigated the structure of the hydrogen-covered phase with no thermal activation ( $T < 180$  K), suspecting that this phase may be a precursor of the above-mentioned transition at higher temperatures. We recall that the clean surface, Ir(100)-(5×1)-hex, is characterized by a hexagonally close-packed top layer which is atomically denser by 20% than the layers beneath.<sup>4</sup> This model of Ir(100)-(5×1)-hex has been confirmed by quantitative low-energy electron diffraction (LEED),<sup>5–10</sup> density functional theory (DFT) calculations,<sup>11–13</sup> and scanning tunneling microscopy (STM).<sup>10,14</sup> Due to the relative excess of atoms in the top layer, this layer is buckled by as much as 0.55 Å inducing bucklings even down to the fifth layer with decreasing magnitude.<sup>10</sup> The basic structure is shown in Fig. 1.

Upon hydrogen adsorption below 180 K, the LEED pattern remains (5×1)-periodic and the ratio of energy-

averaged intensities of fractional-order beams relative to those of integer-order ones undergoes very little modification. However, the  $I(E)$  spectra do show significant changes (see below). For this reason, it has been suggested<sup>1</sup> that the quasihexagonal reconstruction is essentially intact in this Ir(100)-(5×1)-hex-H phase, yet with significant modifications. We aim to reveal both these modifications and the hydrogen adsorption sites by quantitative low-energy electron diffraction (LEED) combined with density functional theory (DFT) calculations. The task is demanding because hydrogen has—in the presence of scatterers as strong as iridium—only a very faint effect on LEED spectra. So, on the one hand it is not necessary to consider the large number of possible configurations of H atoms, which makes it pos-

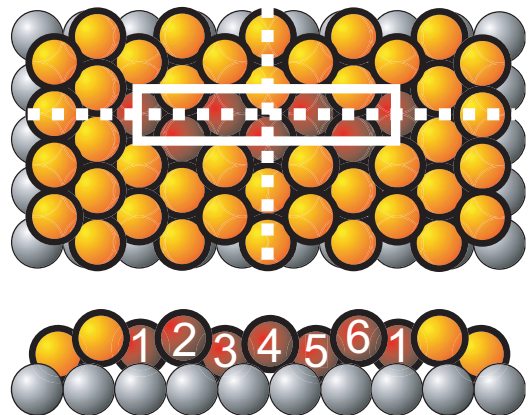


FIG. 1. (Color online) Top and side view ball model of clean Ir(100)-(5×1)-hex with the (5×1) unit cell and the two mirror planes indicated by full and broken lines, respectively.

sible to solve the substrate structure by conventional automated LEED methods. On the other hand, LEED cannot retrieve the hydrogen positions unambiguously. Yet, this is possible by DFT—but only when the hydrogen saturation coverage is known. The latter can in principle be accessed by total energy calculations, but without the consideration of the kinetics (including dissociation) this must be regarded as only an estimate. Fortunately, the *combined* application of quantitative LEED and DFT solves the problem in total: The substrate structure determined by LEED can be taken as a fingerprint of the hydrogen adsorption scenario. It can be used for calibration of the coverage in the DFT calculations with simultaneous determination of the corresponding hydrogen adsorption geometry.

## II. EXPERIMENTAL

The experiments were performed in an apparatus equipped with LEED optics and an STM as described in detail earlier.<sup>1</sup> Also, the same Ir(100) crystal was used which, due to its excellent alignment accuracy ( $\leq 0.1^\circ$ ), exhibits huge terraces of up to micrometer size. Sample sputtering by 2 keV Ar<sup>+</sup> ions followed by annealing at 1300 K in an O<sub>2</sub> atmosphere of  $2 \cdot 10^{-7}$  mbar produced a sharp and low-background  $(5 \times 1)$  diffraction pattern with equally weighted orthogonal domains and no impurities detectable by Auger electron spectroscopy (AES). Upon hydrogen adsorption at low temperatures ( $T < 180$  K, 100 L H<sub>2</sub>) this Ir(100)- $(5 \times 1)$ -hex phase transforms to the Ir(100)- $(5 \times 1)$ -hex-H, i.e., a phase with the  $(5 \times 1)$  symmetry of the LEED pattern unchanged.

LEED intensity data were taken for both the reconstructed clean and hydrogen-saturated surfaces at normal incidence of the primary beam and the sample at about 100 K using a charge-coupled device (CCD) video camera operated under computer control as described in detail earlier.<sup>15,16</sup> Full diffraction images were stored on hard disk in steps of 0.5 eV between 20 and 500 eV allowing for total measuring times of about 15 min independent of the complexity of the patterns. The intensity spectra of individual beams resulted from off-line evaluation whereby symmetrically equivalent beams were averaged as usual. The energy width of 36 accumulated inequivalent beams amounts to  $\Delta E \cong 10\,000$  eV. It appears that the energy-averaged intensity level of fractional order beams relative to integer order beams ( $r = \langle I_{frac} \rangle / \langle I_{int} \rangle$ ) is nearly the same for both phases, i.e.,  $r_{hex} \approx r_{hex-H} \approx 0.6$ . The overall spectral shapes of the different spectra remain but there are also clear differences as illustrated in Fig. 2 for a selected beam (the Pendry  $R$  factor<sup>17</sup> between the two phases as averaged over all beams is  $R_p = 0.37$ ).

Beside the LEED experiments we also applied thermal desorption spectroscopy (TDS) in order to estimate the amount of hydrogen adsorbed. The entrance of the quadrupole mass spectrometer (VG, SX 200) was positioned right in front of the sample to avoid acceptance of desorbing hydrogen from the sample holder. The TD spectra were recorded by applying a constant temperature increase with time (1 K/s) and integrated to give the total coverage by calibration with the value obtained recently for hydrogen ad-

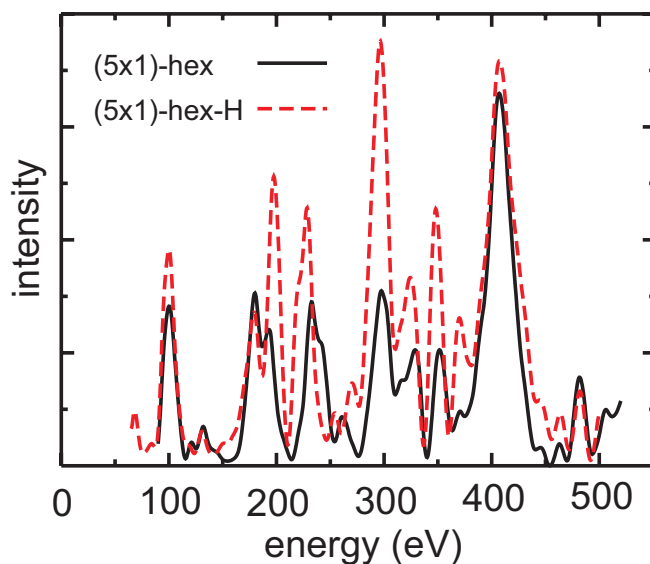


FIG. 2. (Color online) Comparison of LEED intensity spectra of the  $(6/5\ 0)$  beam of the two phases Ir(100)- $(5 \times 1)$ -hex and Ir(100)- $(5 \times 1)$ -hex-H.

sorption on the unreconstructed surface of Ir(100).<sup>18</sup> It turns out that hydrogen desorbs under the LEED beam so that the saturation value in the presence of the beam is below 0.8 ML, i.e., smaller than that at thermal equilibrium.

## III. COMPUTATIONAL METHODOLOGY

### A. LEED intensity calculations

For the LEED intensity calculations up to electron energies of 500 eV relativistically computed and spin-averaged phase shifts were used with angular momentum quantum numbers up to  $l_{max} = 12$  during the structural search and up to  $l_{max} = 14$  for the final structural refinement. Electron attenuation was simulated by, as usual, an imaginary part of the inner potential, here a constant value of  $V_{0i} = 5.0$  eV as applied also for the analysis of the clean surface.<sup>10</sup> The real part of the inner potential,  $V_{0r}$ , was allowed to vary with energy because of the large energy range covered and in view of the energy dependence of the exchange-correlation potential. The dependence was assumed to be linear of the form  $V_{0r} = A + B \cdot E$ . The value  $B = -0.008$  was found to give the best fit to experiment. The value of  $A$  was varied during the course of the theory-experiment fit. The best-fit value for the thermal-vibration amplitude was 0.07 Å.

The structure determination was made in two steps. In the first one we wanted to make sure that—as reflected by the intensity ratio—the  $(5 \times 1)$ -hex-H phase corresponds indeed to a quasihexagonal surface reconstruction similar (though not identical) to that of the clean surface. For that rough test we used the quasidynamical approximation<sup>19</sup> (with in-plane multiple scattering neglected to save computer time) which had been already successfully applied to the clean surface.<sup>8</sup> A global search algorithm based on simulated annealing<sup>20</sup> was used at this stage to find the probability distribution of atoms within the top hexagonal layer with the substrate at-

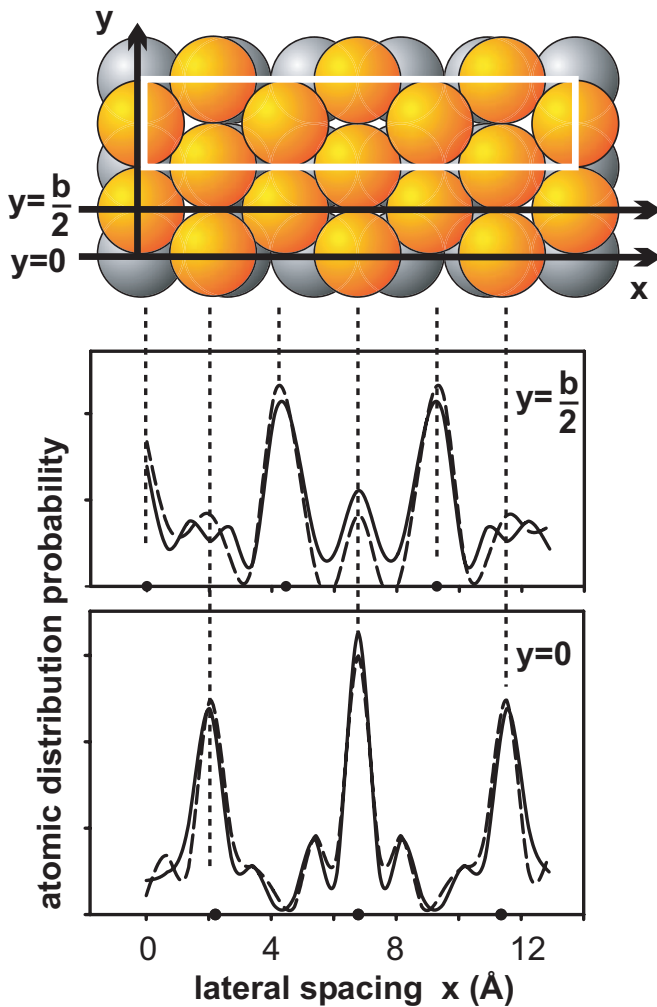


FIG. 3. (Color online) Probability distributions of atoms along  $y=0$  and  $y=b/2$  in the top layer, as retrieved by a global simulated annealing algorithm for clean Ir(100)-(5 $\times$ 1)-hex (dotted line) and the low-temperature Ir(100)-(5 $\times$ 1)-hex-H phase (solid line). The  $x$  and  $y$  axes are also shown. The length of the short side of the unit cell is denoted by  $b$ . Dots on the  $x$  axes indicate the expected positions of atoms in the quasihexagonal phase.

oms fixed at their bulk positions. Due to the symmetry with respect to the mirror plane parallel to the long side of the unit cell (see Fig. 1), the atoms were assumed to lie only along one of the two lines,  $y=0$  and  $y=b/2$  given in the top panel of Fig. 3, where  $b=2.715$  Å is the length of the short side of the (5 $\times$ 1) unit cell. The comparison of the resulting probability distributions for the clean (5 $\times$ 1)-hex and the low temperature (5 $\times$ 1)-hex-H phase is displayed in the lower panel of Fig. 3. Clearly, the two distributions are essentially the same, implying that the quasihexagonal structure of clean Ir(100)-(5 $\times$ 1)-hex is not changed much upon hydrogen adsorption at low temperature, in line also with the similar intensity ratio  $r$  mentioned above. On the other hand, it is obvious that the quasidynamical approximation is not sufficient to describe the structural differences apparent in the spectra of the two phases and we need to go beyond that.

For an adequate intensity calculation we used the perturbation method tensor LEED (TLEED) as described in detail

in the literature.<sup>15,21,22</sup> Two different program packages were applied: The Milwaukee authors of the present paper used the package from the Berkeley group<sup>23</sup> with renormalized forward scattering (RFS) handling the interlayer scattering, and the Erlangen authors used the Erlangen package [TENSERLEED (Ref. 24)] with layer doubling involved for the stacking of layers. Both groups applied the Pendry  $R$  factor ( $R_p$ )<sup>17</sup> for the quantitative comparison of experimental and computed intensity spectra. The best-fit structures found by the two subgroups differ by 0.01 Å at most for the whole set of structural parameters and so there is a single result on which we can concentrate in Sec. IV.

## B. DFT calculations

As indicated above the DFT calculations could not be based on an unambiguous knowledge of the hydrogen (saturation) coverage of the Ir(100)-(5 $\times$ 1)-hex-H structure. Therefore, the calculations had to be performed for different values of hydrogen coverage in steps of 0.2 monolayers [1 H atom per (5 $\times$ 1) unit cell] and for each coverage the energetics concerning the adsorption site(s) and the adsorption-induced changes in the substrate had to be optimized. This is a rather complex procedure and we need only the structural result for the hydrogen saturated surface in the present paper. Therefore, we present the energetics and structures of the whole coverage range in a separate paper<sup>13</sup> and focus here on the structural parameters obtained for saturation coverage. The computational details will also be described in detail in the paper to come, so that we can do with only the essentials here: We applied the projector augmented wave (PAW) method<sup>25,26</sup> of the Vienna *ab initio* simulation Package (VASP).<sup>27-30</sup> The exchange-correlation was treated within the generalized gradient approximation (GGA) according to Perdew *et al.* (PW91).<sup>31</sup> The hydrogen-covered surface was modeled by repeated surface slabs of 9 Ir layers (+1 H layer) of 17.5 Å thickness (+H layer) separated by a vacuum equivalent to a thickness of 5 Ir layers (9.7 Å). The slabs were asymmetric in the sense that hydrogen adsorption and multilayer relaxation were considered only on one side. On the other side, four Ir interlayer spacings were kept fixed (bulklike termination). In order to obtain a clear energy hierarchy of the different adsorbate configurations it was important to correct the adsorption energies for zero-point vibrations.

## IV. RESULTS FOR IR(100)-(5 $\times$ 1)-HEX-H

### A. Substrate structure as determined by LEED

The refined structural search for Ir(100)-(5 $\times$ 1)-hex-H at low temperature was initialized with the established quasihexagonal structure of the clean surface, Ir(100)-(5 $\times$ 1)-hex,<sup>10</sup> as suggested by the results of our preliminary global search. The experimentally observed four-fold symmetry of the diffraction pattern was assumed due to the coexistence of (5 $\times$ 1) and (1 $\times$ 5) domains. As in the case of the clean surface, it was initially assumed that there are mirror planes parallel to the  $x$  and  $y$  axes (see Fig. 1). The atomic coordinates of the top four layers were allowed to

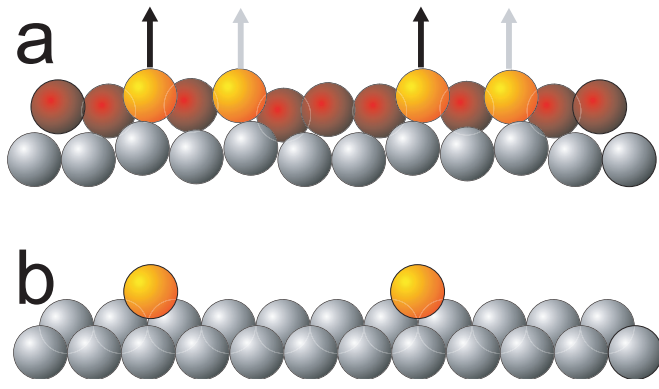


FIG. 4. (Color online) Illustration of the deconstruction process Ir(100)-(5×1)-hex-H (a) → Ir(100)-(5×1)-H (b) according to Ref. 32. Note that no hydrogen atoms are shown.

vary (20 structural parameters) and, as argued above, hydrogen atoms did not need to be included in the calculation. It was found that the optimized structure has an  $R$  factor  $R_p = 0.33$ . This level of theory-experiment agreement appears—given the negligible influence of hydrogen scattering—unacceptable in view of the value achieved for the clean surface ( $R_p = 0.14$ ).<sup>10</sup> Thus, we were faced with a puzzle: On the one hand, our preliminary quasidynamical analysis and the almost unmodified ratio between energy-averaged fractional and integer order beam intensities suggest that the structures of Ir(100)-(5×1)-hex-H and Ir(100)-(5×1)-hex must be similar. On the other hand, the significant elevation of  $R_p$  relative to that for the clean surface suggests that there are corresponding differences.

The clue to the resolution of this puzzle lies in the realization that, in the clean surface, two of the six atoms of the unit cell of the quasi-hexagonal layer are buckled outward by being situated close to atop sites on the underlying layer, two are buckled inward by being close to hollow sites, and two (at bridge sites) are at intermediate heights (see Fig. 1). Yet, as has been described in detail<sup>1,32</sup> and as illustrated in Fig. 4, on annealing of the hydrogen covered hexagonal surface, one top layer atom of the (5×1) unit cell is ejected from that layer to form an adatom, while the layer itself deconstructs back to essentially a standard fcc(100)-type layer. STM investigations found<sup>1</sup> that the ejected atom must be one of the two most protruding atoms in the (5×1) surface unit cell of the quasi-hexagonal layer [bright top layer atoms in Fig. 4(a)]. Yet, with only one of them expelled, the mirror symmetry of the clean surface (with the plane parallel to the short axis of the unit cell) must be broken. This symmetry break may take place during the transition or, alternatively, may be realized already in the hydrogen covered low-temperature phase and so favor one of the formerly equivalent atoms. Thus, the structure before annealing could be some symmetry-lowered precursor of the transition.

As it turns out, this reduction of the symmetry of the unit cell is the key to solving this structure. Of course, to be consistent with the observed symmetry of the diffraction pattern, it is necessary to postulate equally populated domains with unit cells related by this mirror symmetry. In order to test such a model, it was necessary to increase the number of

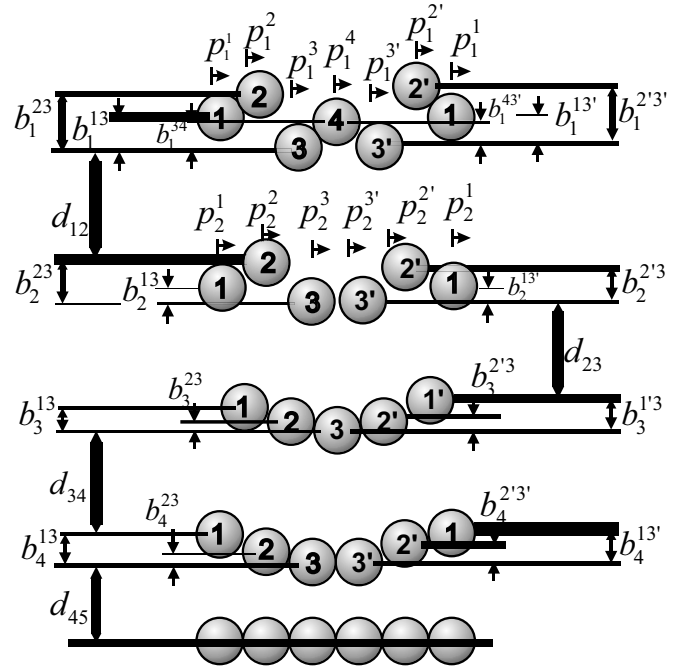


FIG. 5. Parameters describing the substrate structure of Ir(100)-(5×1)-hex-H without assuming a mirror symmetry plane through atom 4 and normal to the paper plane. The in-plane atomic shifts  $p_i^j$  of atoms  $j$  in layer  $i=1,2$  are measured relative to the positions  $x_i^j = a \cdot (j-1)/6$  for the top layer ( $i=1$ ), and for  $j=1, \dots, 6$  and relative to  $x_i^j = a \cdot (j-1)/5$  for the second layer ( $i=2$ ), and for  $j=1, \dots, 5$ , whereby  $a = 5 \cdot a_{Ir} = 13.6 \text{ \AA}$  is the length of the long side of the (5×1) unit mesh. Note that vertical and in-plane atomic shifts are largely exaggerated for clarity.

characterizing structural parameters to 33, raising the question whether or not our data base width is sufficient for their reliable determination. The average full peak width in the  $I(E)$  curves is about  $\Delta E_p \approx 4V_{0i} = 20 \text{ eV}$ . Following Pendry's argument,<sup>17</sup> this suggests that the number of independent data values is  $\Delta E / \Delta E_p \approx 10,000 / 20 = 500$ . Even with a redundancy factor of 3–5, this is still much larger than the number of parameters to be determined, so we are on the safe side.

With a symmetry-breaking model, the  $R$  factor of the optimized structure decreased to  $R_p = 0.16$ , i.e., to about the same quality of fit as achieved for the clean surface. The corresponding best-fit model parameters as defined in Fig. 5 are listed in Table I, and the quality of the best-fit is visually illustrated in Fig. 6 for a selected beam. The differences with respect to the clean surface are illustrated in Fig. 7. This shows that one of the top site Ir atoms is further extruded from the surface by about 0.1 Å upon hydrogen adsorption—consistent with the suspicion that we are dealing with a precursor state for the full extraction of one atom per unit cell in the transition (5×1)-hex-H → (5×1)-H. The other atoms in the top layer are all perturbed to a lesser degree resulting in an asymmetry in the top layer by amplitudes 0.69 and 0.60 Å as compared to the symmetric buckling of 0.55 Å on the clean surface.

Of course, at this point the question arises whether or not the already clean surface, Ir(100)-(5×1)-hex, lacks this mir-

TABLE I. LEED and DFT results for the geometrical parameters (defined in Fig. 5) of the Ir(100)-(5×1)-hex-H phase for a coverage of 0.6 ML hydrogen. Additionally, the center-of-mass spacings  $\bar{d}_{i,i+1}$  between neighboring substrate layers are given, also.

		LEED (Without H)	DFT	LEED (With H)
Hydrogen Layer	$L^{H1-2}$	-	1.88	1.88(fix)
	$L^{H1-3}$	-	1.93	1.93(fix)
	$L^{H2-3}$	-	1.82	1.82(fix)
	$L^{H2-4}$	-	1.94	1.94(fix)
	$L^{H1'-3'}$	-	2.56	2.56(fix)
	$L^{H1'-2'}$	-	1.79	1.79(fix)
1st Iridium Layer	$d_{12}(\text{Å})$	1.87	1.886	1.86
	$\bar{d}_{12}(\text{Å})$	2.26	2.284	2.25
	$b_1^{13}(\text{Å})$	0.32	0.30	0.33
	$b_1^{13'}(\text{Å})$	0.29	0.26	0.29
	$b_1^{23}(\text{Å})$	0.60	0.61	0.60
	$b_1^{2'3'}(\text{Å})$	0.70	0.70	0.69
	$b_1^{34}(\text{Å})$	0.29	0.30	0.29
	$b_1^{3'4}(\text{Å})$	0.26	0.26	0.26
	$p_1^1(\text{Å})$	-0.16	-0.15	-0.16
	$p_1^2(\text{Å})$	-0.21	-0.22	-0.21
	$p_1^{2'}(\text{Å})$	-0.07	-0.08	-0.07
	$p_1^3(\text{Å})$	-0.17	-0.18	-0.17
	$p_1^{3'}(\text{Å})$	-0.02	-0.03	-0.01
	$p_1^4(\text{Å})$	-0.03	-0.01	-0.02
2nd Iridium Layer	$d_{23}(\text{Å})$	1.75	1.778	1.74
	$\bar{d}_{23}(\text{Å})$	1.88	1.901	1.88
	$b_2^{13}(\text{Å})$	0.10	0.06	0.09
	$b_2^{13'}(\text{Å})$	0.12	0.10	0.11
	$b_2^{23}(\text{Å})$	0.12	0.12	0.12
	$b_2^{2'3'}(\text{Å})$	0.15	0.13	0.15
	$p_2^1(\text{Å})$	-0.01	-0.01	0.00
	$p_2^2(\text{Å})$	+0.03	+0.03	+0.03
	$p_2^{2'}(\text{Å})$	-0.04	-0.04	-0.03
	$p_2^3(\text{Å})$	+0.01	+0.02	+0.01
$p_2^{3'}(\text{Å})$	-0.02	-0.01	-0.02	
3rd Iridium Layer	$d_{34}(\text{Å})$	1.81	1.860	1.82
	$\bar{d}_{34}(\text{Å})$	1.92	1.956	1.93
	$b_3^{13}(\text{Å})$	0.12	0.10	0.12
	$b_3^{1'3}(\text{Å})$	0.13	0.11	0.13
	$b_3^{23}(\text{Å})$	0.08	0.07	0.08
	$b_3^{2'3}(\text{Å})$	0.06	0.04	0.06
4th Iridium Layer	$d_{45}(\text{Å})$	1.88	1.900	1.88
	$\bar{d}_{45}(\text{Å})$	1.91	1.937	1.91
	$b_4^{13}(\text{Å})$	0.03	0.05	0.04
	$b_4^{13'}(\text{Å})$	0.00	0.06	0.00
	$b_4^{23}(\text{Å})$	0.02	0.03	-0.01
	$b_4^{2'3'}(\text{Å})$	0.03	0.03	0.02

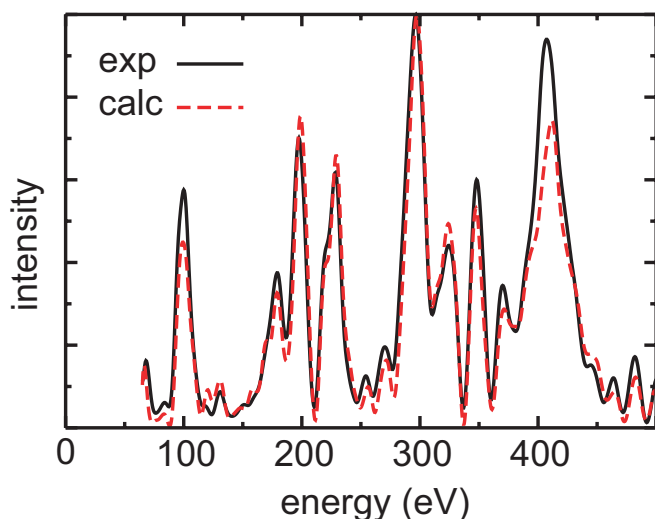


FIG. 6. (Color online) Comparison of the experimental and best-fit calculated spectra for the (6/5 0) beam of Ir(100)-(5 × 1)-hex-H.

ror symmetry. Indeed, to our knowledge all earlier LEED (and DFT) analyses imposed this mirror symmetry as a prerequisite, resulting in a best-fit  $R$  factor of  $R=0.144$  (our work<sup>10</sup>). Therefore, we performed an intensity analysis for the clean surface with this particular mirror symmetry relaxed. In this case, the  $R$  factor improved only marginally

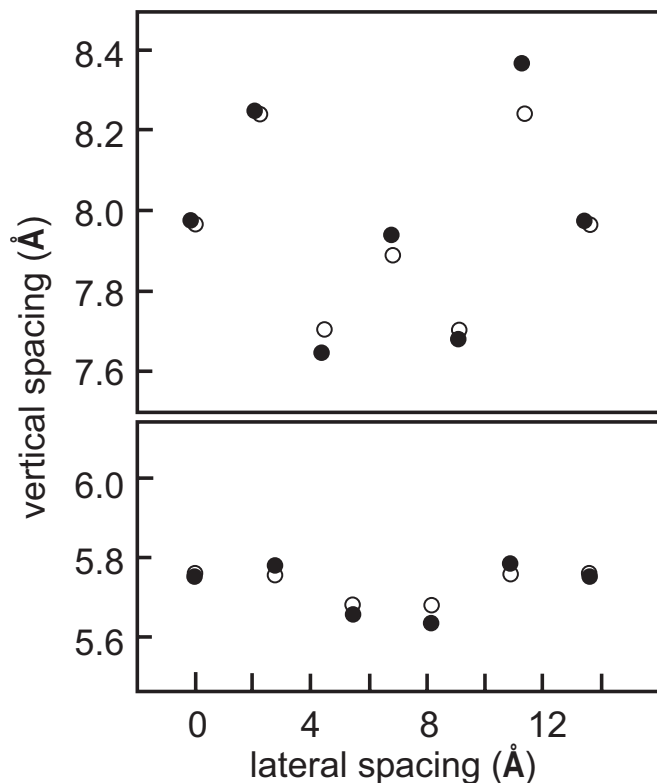


FIG. 7. Illustration of the atomic shifts for the first two iridium substrate layers upon hydrogen adsorption. Empty (solid) circles denote the atom positions before (after) hydrogen adsorption. The ordinate spacing are with respect to the position of the 5th substrate layer.

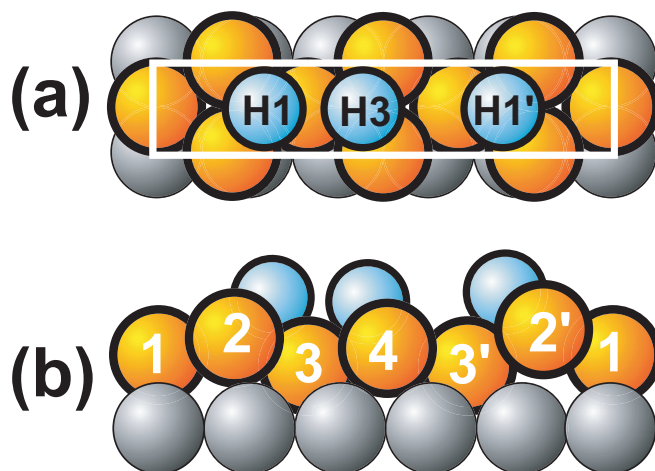


FIG. 8. (Color online) Ball model of the hydrogen adsorption geometry in the Ir(100)-(5 × 1)-hex-H phase in top (a) and side (b) view.

( $\Delta R=-0.006$ ), of magnitude less than the reliability (0.009) of the  $R$  factor. This marginal lowering of the  $R$  factor is probably mainly due to the increase in the number of adjustable parameters in the nonsymmetric model, and was accompanied by a negligible change in atomic positions. We also performed DFT calculations which, unlike our earlier ones,<sup>18</sup> did not enforce the mirror symmetry. The total energy decreased by only about 0.2 meV per (5 × 1) unit cell and the atomic positions remained the same again to within 0.01 Å. All these deviations are well within the error limits of the methods applied. So, the results described of both LEED and DFT confirm that the mirror symmetry is broken only by the hydrogen adsorption.

### B. Hydrogen positions as determined by DFT

As outlined in the introduction, the coverage and adsorption geometry of hydrogen atoms promise to be determined by DFT when the substrate structure retrieved by quantitative LEED serves as a framework for determining the coverage. This is because for the correct coverage and geometry DFT must reproduce also the correct substrate structure. So, the coverage was varied in steps of 0.2 ML and for each step all reasonable adsorption sites—as threefold coordinated hollow, twofold bridge, and onefold top sites—were tried as starting points. This was followed by allowing atomic relaxations in the substrate as well as off the ideally coordinated sites for hydrogen until the energy minimum was found under the constraint that the substrate structure is close to the LEED result (closer than 0.1 Å). These extensive efforts identified clearly that the coverage is 0.6 ML. Even more, as will be described in a separate paper,<sup>13</sup> the precise knowledge of the substrate structure by LEED allowed the discarding of one of two energetically close structures at that coverage and to identify the hydrogen adsorption geometry displayed in Fig. 8. The loss of the former vertical mirror symmetry plane (see Fig. 1) clearly shows up, as the middle hydrogen atom does not adsorb within that plane. As a consequence, an asymmetric buckling is indeed induced.

The structural parameters calculated by DFT for the substrate corresponding to the minimum energy of the 0.6 ML phase are compared with the LEED result in the middle column of Table I. It is apparent that the substrate geometries retrieved by DFT and LEED compare impressively well: For 27 of the 33 parameters the deviations are not larger than 0.02 Å. In the first substrate layer, the maximum deviation is 0.03 Å, in the second layer 0.04 Å, in the third layer 0.05 Å, and in the fourth layer 0.06 Å. To some extent this might reflect the decreasing accuracy of LEED with increasing sample depth, but certainly also limitations with respect to DFT are involved (note that we compare absolute quantities).

Table I also provides the hydrogen positions as retrieved by DFT. They are given in terms of bond lengths  $L$  to the neighboring iridium atoms whereby for the different atoms the notation displayed in Fig. 8 is used (e.g.,  $L^{H1-2}$  is the bond length of H atom  $H1$  to Ir atom number 2). As the structural relaxation was started with hydrogen adsorbed in hollow (=H) sites we denote the sites by  $H1$ ,  $H1'$ , and  $H3$  though they move away from these ideal sites in the relaxation process. This is obvious from the fact that  $L^{H1-2} < L^{H1-3}$ ,  $L^{H3-3} < L^{H3-4}$ , and  $L^{H1'-2'} < L^{H1'-3'}$ , i.e., all hydrogen atoms are shifted toward bridge positions without, however, really assuming ideal bridge positions. Hydrogen atom  $H1'$  is nearest to bridge position (the lateral distance from it is 0.38 Å). Accordingly, because of this near twofold coordination it has extracted the number 2' iridium atom out of the surface by a much larger amount than atoms number 2 and number 4, consistent with the asymmetric buckling already mentioned. The difference in the surface protrusion of atoms numbers 2 and 2' is as large as  $\Delta_{22'} = (b_1^{2'3'} - b_1^{13'}) - (b_1^{23} - b_1^{13}) = 0.13$  Å.

The eventual knowledge of the hydrogen positions encouraged us to carry out an additional LEED calculation with hydrogen atoms fixed at their DFT positions and their scattering included. Not surprisingly it was found that this has little effect either on the  $R$  factor (which reduced by an amount less than the accuracy of the  $R$  factor, i.e., by less than 0.01) or on the positions of Ir atoms ( $\leq 0.01$  Å). The resulting substrate parameters are shown in the last column of Table I.

## V. DISCUSSION AND CONCLUSION

We have determined the full crystallographic structure of the Ir(100)-(5×1)-hex-H phase, stable at low temperature (<180 K). It was found that adsorption of 0.6 ML of hydrogen atoms leads to the breaking of one of the mirror symmetries of the unit cell of the Ir(100)-(5×1)-hex clean surface. Only by giving up this mirror symmetry could a satisfying theory-experiment fit be achieved in LEED (equivalent to a decrease of the Pendry  $R$  factor from 0.33 to 0.16). The positions of the hydrogen adatoms—which induce the symmetry break—could only be determined by the combined application of quantitative LEED and DFT. With LEED being almost insensitive to hydrogen in the presence of the strong iridium scatterers it can only determine the substrate structure reliably. Yet, this could be used by DFT to identify

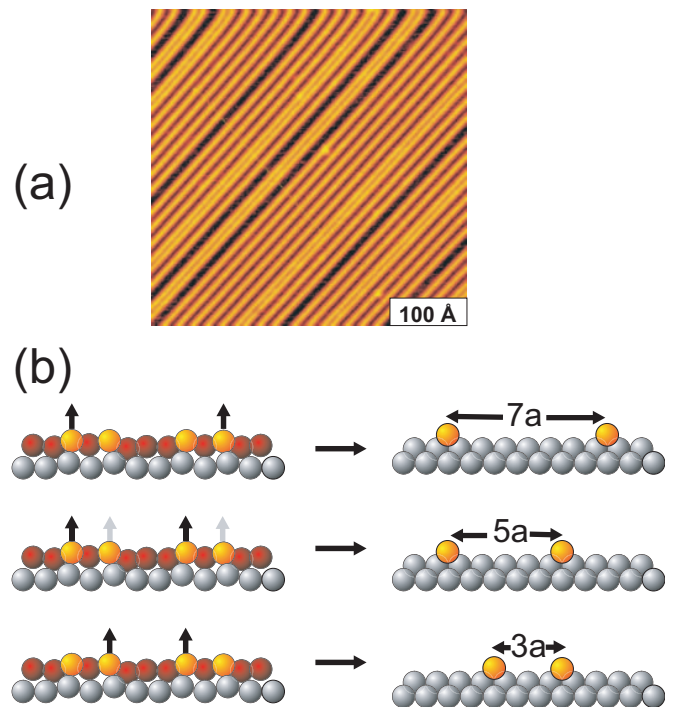


FIG. 9. (Color online) (a) STM image of the phase Ir(100)-(5×1)-H (as taken from Ref. 1) and (b) possible spacings of atomic iridium wires ejected to the surface in the temperature activated transition Ir(100)-(5×1)-hex-H → Ir(100)-(5×1)-H.

the hydrogen saturation coverage (under the presence of the electron beam) which is hard to access accurately. Only for the real coverage and by calculating for that the real hydrogen adsorption geometry can DFT quantitatively reproduce the substrate structure found experimentally by quantitative LEED. LEED and DFT agree to within crystallographic accuracy.

We have described the combined application of quantitative LEED and DFT to establish that hydrogen adsorbs on Ir(100)-(5×1)-hex such as to make previously protruding top layer iridium atoms (numbers 2 and 2') protrude even more. However, the strongest effect is on atom number 2' [the atom in the half of the (5×1) unit cell with only one H adsorbed, cf. Fig. 8]. We interpret this as a precursor state for the ejection of atom number 2' in the hydrogen induced phase transition at higher temperature (>180 K) leading to atomically thin wires made up of these atoms.<sup>1</sup> This means that the spontaneous symmetry breaking by the ejection of only one of the protruding atoms of the unit cell is induced by the hydrogen adsorption and not by thermal activation of the transition. A crucial test for that interpretation is the mutual arrangement of iridium wires after the transition is completed. In Fig. 9(a) the corresponding STM image is displayed (taken from Ref. 1). It appears that the spacings of the wires (in multiples of the in-plane lattice parameter of Ir,  $a_{Ir} = 2.715$  Å) are dominantly (70%)  $5a_{Ir}$ , but also spacings  $3a_{Ir}$  and  $7a_{Ir}$  appear with equal weight (15%). On balance this means that one Ir atom per (5×1) unit cell is ejected to form a surface adatom, so that the 20% atoms additionally accommodated in the hexagonal layer are removed and the remaining atoms can reorder to a bulklike layer as has been

proved quantitatively.<sup>1</sup> This is fully in line with our precursor model according to which one, and only one, atom per unit cell is ejected. It is also in line with the dominant appearance of the spacing  $5a_{Ir}$ , which means that—predominantly—the same (left or right) half of the unit cell in a given domain is singly occupied by hydrogen, i.e., the most protruding and eventually ejected Ir atom is only in this half as indicated in the middle frame of Fig. 9(b). This means that neighboring unit cells are coupled accordingly, and it is reasonable to assume that this coupling is mediated *via* the asymmetric and hydrogen-induced substrate buckling. On the other hand, the coupling is not strong enough to be strictly enforced, in particular as the buckling amplitudes are in the range of thermal vibration amplitudes. So, it can occur that a singly occupied right-hand unit cell half is followed by a left-hand one so that the spacing of the resulting ejected nanowires wires is  $3a_{Ir}$

[lower frame of Fig. 9(b)]. If it is the other way round, the spacing becomes  $7a_{Ir}$  [upper frame of Fig. 9(b)]. This easy and consistent interpretation of all experimental and theoretical findings unequivocally proves that the low-temperature Ir(100)-(5×1)-hex-H phase with its spontaneously broken mirror symmetry is indeed a precursor state for the lifting of the hexagonal reconstruction taking place at higher temperature.

#### ACKNOWLEDGMENTS

H.C.P. and D.K.S. (P.I.) acknowledge support for this work from the U.S. Department of Energy (Grant No. DE-FG02-84ER45076). The Erlangen authors are grateful for financial support through Deutsche Forschungsgemeinschaft.

\*Corresponding author. Email address: dksaldin@uwm.edu

<sup>1</sup>L. Hammer, W. Meier, A. Klein, P. Landfried, A. Schmidt, and K. Heinz, Phys. Rev. Lett. **91**, 156101 (2003).

<sup>2</sup>A. Klein, A. Schmidt, L. Hammer, and K. Heinz, Europhys. Lett. **65**, 830 (2004).

<sup>3</sup>K. Heinz, L. Hammer, A. Klein, and A. Schmidt, Appl. Surf. Sci. **237**, 519 (2004).

<sup>4</sup>A. Ignatiev, A. V. Jones, and T. N. Rhodin, Surf. Sci. **30**, 573 (1972).

<sup>5</sup>M. A. Van Hove, R. J. Koestner, P. C. Bibérian, L. L. Kesmodel, I. Bartóš, and G. A. Somorjai, Surf. Sci. **103**, 189 (1981).

<sup>6</sup>E. Lang, K. Müller, K. Heinz, M. A. Van Hove, R. J. Koestner, and G. A. Somorjai, Surf. Sci. **127**, 347 (1983).

<sup>7</sup>W. Moritz, F. Müller, D. Wolf, and H. Jogodzinski, in *Book of Abstracts of the 9th Vacuum Congress and 5th International Conference on Solid Surfaces*, edited by J. L. de Segovia (A.S.E.V.A., Madrid, 1983), p. 70.

<sup>8</sup>N. Bickel and K. Heinz, Surf. Sci. **163**, 435 (1985).

<sup>9</sup>K. Johnson, Q. Ge, S. Titmuss, and D. A. King, J. Chem. Phys. **112**, 10460 (2000).

<sup>10</sup>A. Schmidt, W. Meier, L. Hammer, and K. Heinz, J. Phys.: Condens. Matter **14**, 12353 (2002).

<sup>11</sup>Q. Ge, D. A. King, N. Marzari, and M. C. Payne, Surf. Sci. **418**, 7461 (1989).

<sup>12</sup>D. Spišák and J. Hafner, Surf. Sci. **546**, 27 (2003).

<sup>13</sup>D. Lerch, S. Müller, L. Hammer, and K. Heinz, Phys. Rev. B **74**, 075426 (2006).

<sup>14</sup>G. Gilarowsky, J. Méndez, and H. Niehus, Surf. Sci. **448**, 290

(2000).

<sup>15</sup>K. Heinz, Rep. Prog. Phys. **58**, 637 (1995).

<sup>16</sup>K. Heinz and L. Hammer, Z. Kristallogr. **213**, 615 (1998).

<sup>17</sup>J. B. Pendry, J. Phys. C **13**, 937 (1980).

<sup>18</sup>D. Lerch, A. Klein, A. Schmidt, S. Müller, L. Hammer, K. Heinz, and M. Weinert, Phys. Rev. B **73**, 075430 (2006).

<sup>19</sup>M. A. Van Hove, W. H. Weinberg, and C.-M. Chan, *Low-Energy Electron Diffraction* (Springer, Berlin, 1986).

<sup>20</sup>H. C. Poon and D. K. Saldin (unpublished).

<sup>21</sup>P. J. Rous, J. B. Pendry, D. K. Saldin, K. Heinz, K. Müller, and N. Bickel, Phys. Rev. Lett. **57**, 2951 (1986).

<sup>22</sup>P. J. Rous, Surf. Sci. **39**, 3 (1992).

<sup>23</sup>A. Barbieri and M. A. Van Hove, Symmetrized Automated Tensor LEED Package, available from M. A. Van Hove.

<sup>24</sup>V. Blum and K. Heinz, Comput. Phys. Commun. **134**, 392 (2001).

<sup>25</sup>G. Kresse and D. Joubert, Phys. Rev. B **59**, 1758 (1999).

<sup>26</sup>P. E. Blöchl, Phys. Rev. B **50**, 17953 (1994).

<sup>27</sup>G. Kresse and J. Hafner, Phys. Rev. B **47**, R558 (1993).

<sup>28</sup>G. Kresse and J. Hafner, J. Phys.: Condens. Matter **6**, 8245 (1994).

<sup>29</sup>G. Kresse and J. Furthmüller, Phys. Rev. B **54**, 11169 (1996).

<sup>30</sup>G. Kresse and J. Furthmüller, Comput. Mater. Sci. **6**, 15 (1996).

<sup>31</sup>J. P. Perdew, J. A. Chevary, S. H. Vosko, K. A. Jackson, M. R. Pederson, D. J. Singh, and C. Fiolhais, Phys. Rev. B **46**, 6671 (1992).

<sup>32</sup>K. Heinz and L. Hammer, Z. Phys. Chem. **218**, 997 (2004).